ELSEVIER

Marine Geology 179 (2001) 105–119

MARINE GEOLOGY
INTERNATIONAL JOURNAL OF MARINE GEOLOGY, GEOCHEMISTRY AND GEOPHYSICS

www.elsevier.nl/locate/margeo

Seasonal variation of sediment deposition in the Hudson River estuary

Jonathan D. Woodruff, W. Rockwell Geyer*, Christopher K. Sommerfield, Neal W. Driscoll

Department of Applied Ocean Physics and Engineering, Woods Hole Oceanographic Institution, 384 Woods Hole Road, Woods Hole, MA 02543, USA

Received 4 July 2000; accepted 8 May 2001

Abstract

During and following the spring freshet, rapid rates of sediment deposition were observed in the Hudson River estuary. Side-scan sonar surveys and sediment coring studies revealed a large amount of spatial variability in sedimentation within the estuary and a distinct seasonal progression. During the freshet, sediment was deposited in the seaward reaches of the estuary. In the two-month period after the freshet, this sediment was eroded and sedimentation occurred 10–30 km further landward at the estuarine turbidity maximum (ETM) zone. The thickness of the new freshet deposit was as great as 40 cm in the ETM, indicating intense trapping and rapid deposition. The location of this depocenter corresponded to a frontal zone, where water column observations and modeling studies have indicated enhanced sediment trapping. The mass of the new deposits was estimated at 300 000 metric tons during both 1998 and 1999, with similar spatial distributions. In 1998 the estimated fluvial input was 560 000 metric tons, significantly greater than the 120 000 metric tons estimated for 1999. Thus, the mass of the observed deposits appear to be more influenced by the redistribution of sediment within the estuary due to seasonal variations in erosion–deposition conditions, rather than by the direct input of sediment from the watershed.

Keywords: Hudson River estuary; Estuaries; Turbidity maximum; Beryllium; Suspended sediment; Seasonal variations

1. Introduction

Estuaries are known to be effective traps for sediment entering them (Glangeaud, 1938; Postma, 1967; Meade, 1969). Most estuaries exhibit a region of elevated suspended sediment concentrations, the estuarine turbidity maximum (ETM), where the flow regime focuses suspended sediment into a particular region, usually near the landward end of the salinity intrusion. A number of different trapping mechanisms can support an ETM including: the convergence of residual flow in estuarine bottom-waters (Postma, 1967); tidal asymmetry (Allen et al., 1980); the reduction in fluvial energy (Nichols et al., 1991); and salinity-induced sediment flocculation (Postma, 1967; Gibbs et al., 1989; Lick and Huang, 1993). Within stratified environments, the occurrence of a salinity front has also been found to intensify the trapping of suspended sediment (Geyer, 1993; Jaeger and Nittrouer, 1995; Huan-ting et al., 1982).

In addition, changes in freshwater outflow can affect estuarine sediment trapping processes, change

* Corresponding author. Tel.: +1-508-289-2868; fax: +1-508-457-2194.

E-mail address: rgeyer@whoi.edu (W.R. Geyer).

0025-3227/01/$ - see front matter
PII: S0025-3227(01)00182-7

the position of the ETM, and alter patterns of sediment deposition (Nichols, 1977; Migniot, 1971; Grabemann et al., 1997). Migniot (1971) showed that the sediment trapping zone of the macrotidal Gironde estuary varied in position by as much as 70 km due to changes in river outflow. This variation resulted in a shifting zone of sediment accumulation, with seasonal accumulation rates of 1 m or more. Grabemann et al. (1997) demonstrated that the location of the ETM in the Tamar and Weser estuaries also exhibited large variations in position as a result of variations in river outflow. Based on changes in the spatial patterns of sediment re-suspension, Grabemann et al. (1997) inferred that there were seasonal movements of an easily eroded pool of bed sediment, although no direct measurements were taken of this surficial layer.

The Hudson River estuary is located on the northeast coast of the United States and empties into the Atlantic Ocean through New York Harbor at its mouth (Fig. 1). An ETM is found on the west side of the Hudson channel, 10–20 km north from where the Hudson joins New York Harbor at the Battery (Hirschberg and Bokuniewicz, 1991; Geyer, 1995; Geyer et al., 1998). Peak near-bed suspended sediment concentrations can exceed 2000 mg/l within this ETM region, much larger than the 20–40 mg/l observed for most of the estuary (Hirschberg and Bokuniewicz, 1991; Geyer, 1995; Geyer et al., 2001). Underlying the ETM is a shoal consisting of fine-grained sediment (Coch, 1986; Flood and Bokuniewicz, 1986). Sedimentation rates within this shoal are among the highest in the estuary, ranging from 10 to 30 cm/yr averaged on a 5 to 10 year timescale, one to two orders of magnitude higher than rates found elsewhere in the estuary (Olsen et al., 1981).

Freshwater inflow is contributed to the Hudson River estuary primarily by the Mohawk and Upper Hudson Rivers, located approximately 250 km upstream from the mouth of the estuary. These rivers account for approximately 70% of the freshwater input and are the major suppliers of fluvial sediment to the estuary (Abood, 1974; Panuzio, 1965). High river discharge events (defined as when the combined flow of the Mohawk and Upper Hudson Rivers exceeds 1200 m^3/s), generally occur in March and April during the spring runoff or freshet. During the freshet suspended sediment loads into the estuary can increase to over 100 000 metric tons per day (Olsen, 1979), two orders of magnitude larger than the long-term mean of 1100 metric tons per day (Woodruff, 1999). In addition to providing most of the fluvial sediment to the estuary, high discharge events also redirect residual bottom water flows from landward to seaward within the ETM and push the salinity intrusion toward the mouth (Abood, 1974; Geyer et al., 1998).

Water column measurements and numerical modeling studies by Geyer et al. (1998) provide some insights into the sediment trapping mechanisms in the Hudson estuary. Results from Geyer et al. (1998) suggest the region of most intense sediment trapping (between 10 and 15 km) is associated with a salinity front that forms during ebb tide, which results in a convergence in bottom water flow and a corresponding convergence of sediment flux, consistent with Postma's (1967) theory. The model of Geyer et al. (1998) also predicts a different trapping process during flood tides, associated with transverse, secondary circulations. In this process, sediment resuspended from the zone of frontal trapping is redeposited in a second trapping zone along the west bank, approximately 10 km north of the frontal trapping zone, between 18 and 25 km. The model of Geyer et al. (1998) also predicts that during high discharge conditions, the convergence of sediment flux occurs closer to the mouth, due to the seaward displacement of the salinity intrusion.

Recent sedimentological studies suggest that there is considerable spatial and temporal variability of deposition within the Lower Hudson River estuary, with isolated pockets of high deposition that appear to occur during and shortly after high river discharge events (Hirschberg et al., 1996; Feng et al., 1998). However, the overall spatial patterns of deposition could not be inferred from these studies, nor was there adequate temporal resolution to determine the depositional response to variations in freshwater flow. One important insight provided by Feng et al. (1999) is that the surficial sediment found in the ETM during the summer has a radionuclide signature consistent with transport from a region of higher salinity, most likely New York Harbor. This evidence suggests that there may be a landward migration of sediment following the freshet.

This study characterizes the spatial distribution of seasonal deposits within the Lower Hudson River

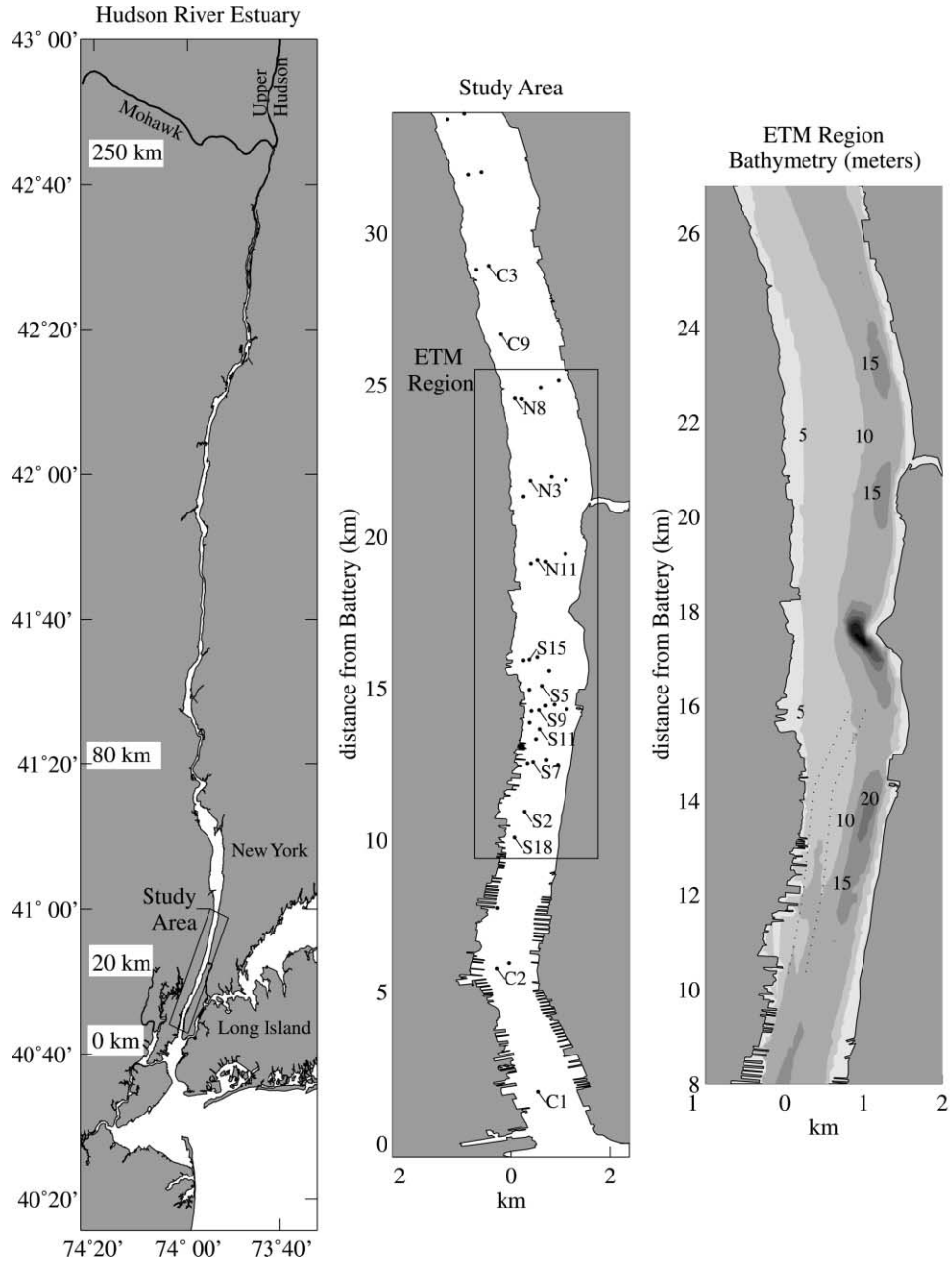

Fig. 1. Map of Hudson River Estuary (left), study area (center) and channel bathymetry for ETM region (right). All positions along the estuary are measured in kilometers northward from the Battery at the southern tip of Manhattan. Coring locations are marked as black dots in center figure with labels next to key coring sites. The Weehawken–Edgewater Channel runs along the west side of the Lower Hudson River estuary between 10 and 15 km (represented by dotted line in bathymetry plot). Depths within this navigation channel were maintained at 9 m until the summer of 1994 (ACOE personal communication).

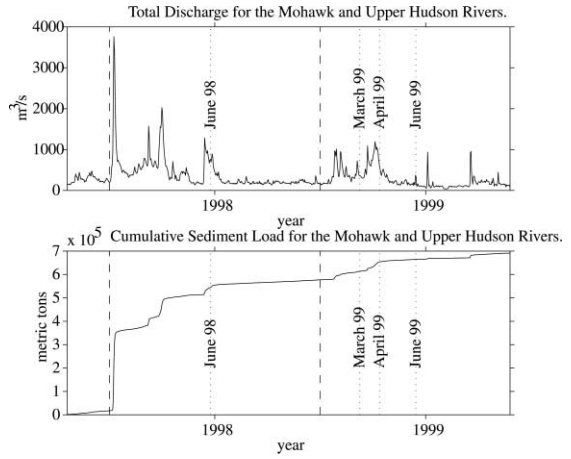

Fig. 2. River discharge for 1998 and 1999 (top panel) and the estimated cumulative sediment load for both years (bottom panel). Sediment load was based on the discharge vs. sediment load power law relationship obtained for the Mohawk and Upper Hudson by Woodruff (1999).

estuary before, during and shortly after the spring freshet. Side-scan sonar is used in conjunction with the collection of numerous sediment cores to: (1) identify longitudinal and transverse depositional patterns within the ETM; (2) quantify the mass of sediment deposition following the spring freshet; and (3) to evaluate the sediment trapping mechanisms identified in the modeling study by Geyer et al. (1998).

2. Environmental conditions

Field work was conducted on the Lower Hudson River estuary in late June of 1998 and during March, April, and June of 1999. The spring freshets of both 1998 and 1999 occurred between late March and mid-April (Fig. 2). Of particular importance in 1998 was an exceptional high discharge event with a 10-year recurrence interval, which occurred during a 5 day period in early January. This event alone contributed approximately 60% of the combined annual suspended load from the Mohawk and the Upper Hudson Rivers, estimated at 560 000 metric tons (Woodruff, 1999). The estimated annual sediment load for 1999 was much lower at 120 000 metric tons. This small sediment load was a result of 1999 having a relatively weak spring freshet and lacking any exceptional discharge events. For both years fluvial sediment input occurred primarily during the winter and spring months, with 96 and 77% of the total annual load contributed between January and April for 1998 and 1999, respectively.

3. Field program and analytical procedures

The 1998 field study took place between June 23 and 25, approximately three months after the spring freshet and six months after the exceptional high discharge event in January (Fig. 2). Fieldwork consisted of a high resolution side-scan survey performed over the ETM region of the Hudson followed by an extensive sediment coring program based on the side-scan results. During 1999, sediment samples were collected in the middle of March, April, and June, coinciding with the beginning, peak, and shortly after the end of the 1999 spring freshet (Fig. 2). Sediment cores were collected from 0 to 35 km, revisiting selected 1998 core sites along with sites to the north and south of the ETM region.

The side-scan survey for the study was divided into two sections, one south of the George Washington Bridge between 10 and 17 km and one north of the Bridge between 18 and 25 km. The data was acquired with a dual frequency, Edge Tech model DF 1000, side-scan sonar operating at 100 and 500 kHz with a swath width of approximately 200 meters. Side-scan sonar data was processed using US Geological Survey, Xsonar and Showimage software as described by Danforth (1997).

A total of 97 sediment cores were collected with a hydraulically dampened, gravity corer (Bothner et al., 1997). This device slowly advanced a one-meter-long, 11 cm diameter core barrel into bottom sediments at approximately 20 cm/s, collecting a representative sample with an undisturbed sediment–water interface. Core barrels were composed of transparent polycarbonate, which allowed for the viewing of core stratigraphy in the field. Each core was described and photographed immediately after retrieval. During the 1999 cruises, a cylindrical resistivity probe, 8 mm in diameter, was used to obtain a down-core depth profile of sediment resistivity shortly after core collection. Subsequently, cores were capped and shipped

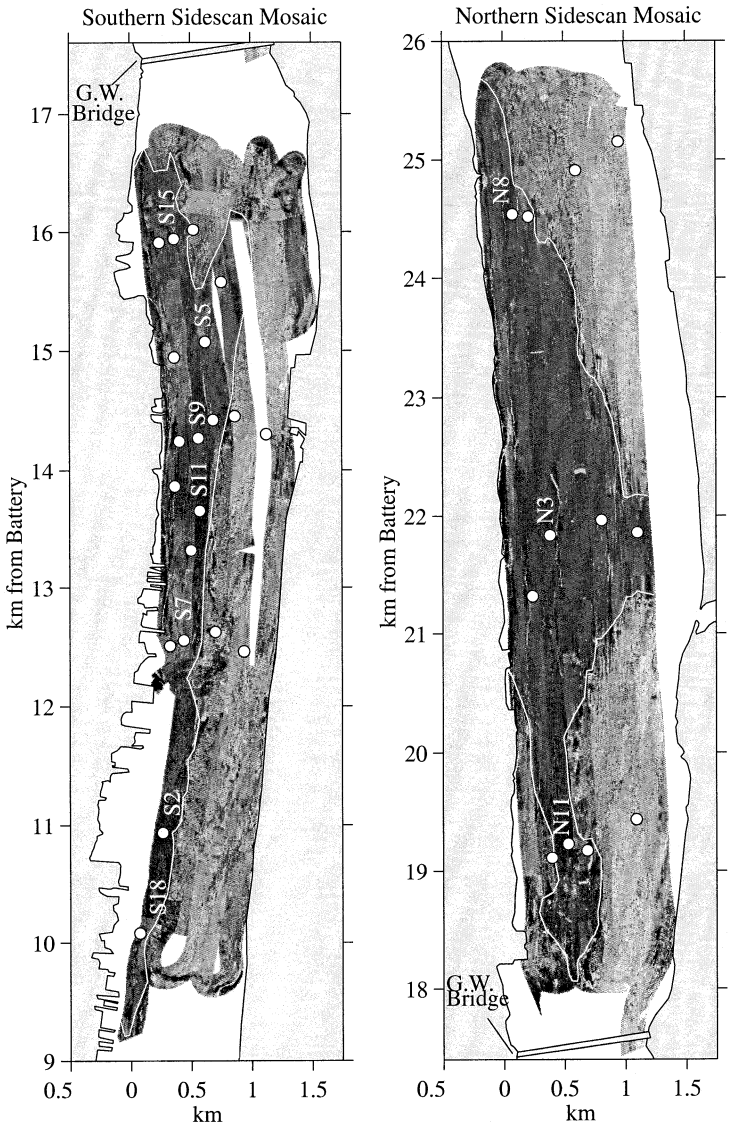

Fig. 3. Sidescan sonar mosaics for southern (left panel) and northern (right panel) sections of the ETM zone. Areas of low side-scan backscatter appear dark in the figure while high side-scan backscatter areas appear light. The thin white line identifies the visual delineation between low and high side-scan backscatter environments. Coring sites are represented by circles with labels located above key sites.

upright to the laboratory, where they were cold stored at 6°C.

In the laboratory, whole-core X-radiographs were taken, and selected cores were subsequently extruded and sampled for grain size, porosity and radionuclide counting. Grain size was determined by wet sieve and pipette analyses as described by Folk (1980). Porosity was determined gravimetrically. These porosity values were used to calibrate the resistivity probe and convert resistivity measurements to porosities using resistivity–porosity relationships described by Dowling (1990) and references therein.

The activity of Beryllium-7 (Be-7) was measured for selected cores to identify recently deposited sediments. Be-7 is a short-lived ($t_{1/2} = 53$ days), cosmogenic radionuclide, which enters estuaries

primarily via atmospheric deposition and runoff (Olsen et al., 1986; Feng et al., 1999). Dissolved Be-7 is scavenged from estuarine waters by suspended particles and, through sedimentation, is delivered to the bed where it decays to extinction. The presence of Be-7 in bottom sediments thus denotes material deposited on a timescale of several months. Be-7 activities were determined for selected cores by gamma spectroscopy of the 477.6 keV photopeak following previously reported methods (Larsen and Cutshall, 1981).

4. Results and interpretation

4.1. Side-scan sonar

The northern and southern side-scan mosaics revealed prominent zones of low backscatter within the ETM (Fig. 3). The two low backscatter zones (darker areas in side-scan record) were located primarily on the shallower, west side of the channel, one to the north and one to the south of the George Washington Bridge. The southern zone (shown in Fig. 3, left panel) began at 9 km, and was coincident with the Weehawken–Edgewater channel until 15 km. North of 15 km, the southern zone widened and divided into two branches, both of which ended around 16 km. The northern low backscatter zone (shown in Fig. 3, right panel), began as a 200-meter wide tongue, extending from 18 to 20 km. North of 20 km, the zone widened until it encompassed nearly the entire width of the channel at 22 km, just upstream of the Harlem River. North of 22 km, the northern zone of low backscatter retreated back towards the west side of the channel, thinning until it terminated at 25 km.

Surficial sediments collected from the northern and southern low backscatter zones were composed of low dry bulk density (0.4–0.8 g/cm^3), fine-grained material ($<$10% sand and gravel). In contrast, cores collected from high backscatter zones (lighter areas in side-scan records) contained a 1 to 10 cm thick, coarse-grained ($>$64% sand and gravel), high dry bulk density (0.9–1.3 g/cm^3) surficial layer. Thus qualitatively, the backscatter intensity in the ETM zone appears to vary directly with both surficial sediment grain size and bulk density.

4.2. Description of sediment cores

The most notable feature of the sediment cores was distinct color stratification, characterized by an olive-brown mud layer (in some cases as much as 40 cm thick), changing abruptly to black sediment (Figs. 4 and 5). This color transition is common for marine and estuarine muds and marks the conversion of iron oxides (olive-brown color) to monosulfides (black color), a consequence of bacterially mediated diagenic reactions (Berner, 1980). At core site S-11, located within the southern low backscatter zone of the ETM, a 25 cm thick layer of olive-brown mud was observed during June of 1998, and 19 cm was observed in June of 1999 (Fig. 4); however this olive-brown layer was absent during the March and April 1999 surveys. Conversely, in the seaward part of the estuary, between the Battery and the ETM, olive-brown mud was observed only during the March and April sampling periods (Fig. 5), and absent during June.

X-radiographs of the cores revealed nearly undisturbed, silt-rich laminations in the olive-brown sediments. Within the ETM, these internal laminae continued below the color change, but in the underlying, black sediments, the X-radiographs had a more mottled appearance, owing to bioturbation and fissuring associated with methane gas expansion (e.g. S-11, Fig. 4). South of the ETM, olive-brown deposits were underlain primarily by much coarser, reworked material (e.g. C-2, Fig. 5).

In cores collected within the two ETM deposits during March and April, 1999, in which the upper, olive-brown layer was thin or absent, X-radiographs indicated disturbed sediment extending nearly to the sediment surface (Fig. 4). Similarly, surficial sediment collected south of the ETM during June, 1999 (e.g. C-2, Fig. 5), contained little to no oxidized mud, and consisted primarily of coarse, reworked material.

Porosities within olive-brown sediment typically ranged from 0.73 to 0.85. Importantly, all the cores showed an abrupt decrease in porosity to under 0.71 below the brown–black boundary (Figs. 4 and 5). In cores for which the surface olive-brown layer were thin or absent (e.g. S-11 during April, 1999, and C-2 during June, 1999), the porosity rapidly decreased within the surficial sediment to values below 0.71.

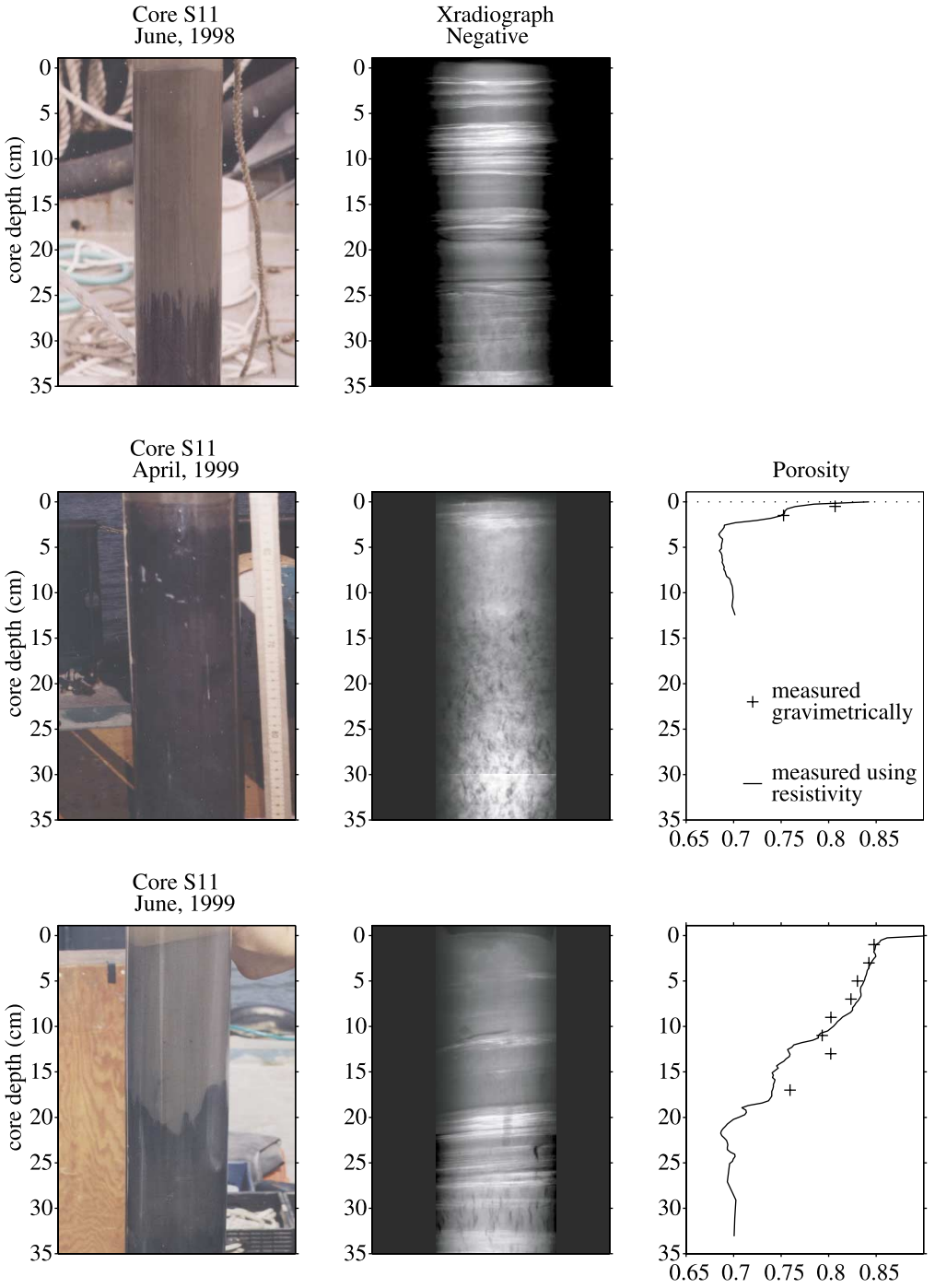

Fig. 4. Photographs, X-radiograph negatives and porosities obtained from sediment cores collected from within the southern deposit at core site S-11: (top panels) two months after the spring freshet of 1998, (middle panels) during the spring freshet of 1999 and (bottom panels) two months after the spring freshet of 1999. Porosities were not obtained during the 1998 sampling period.

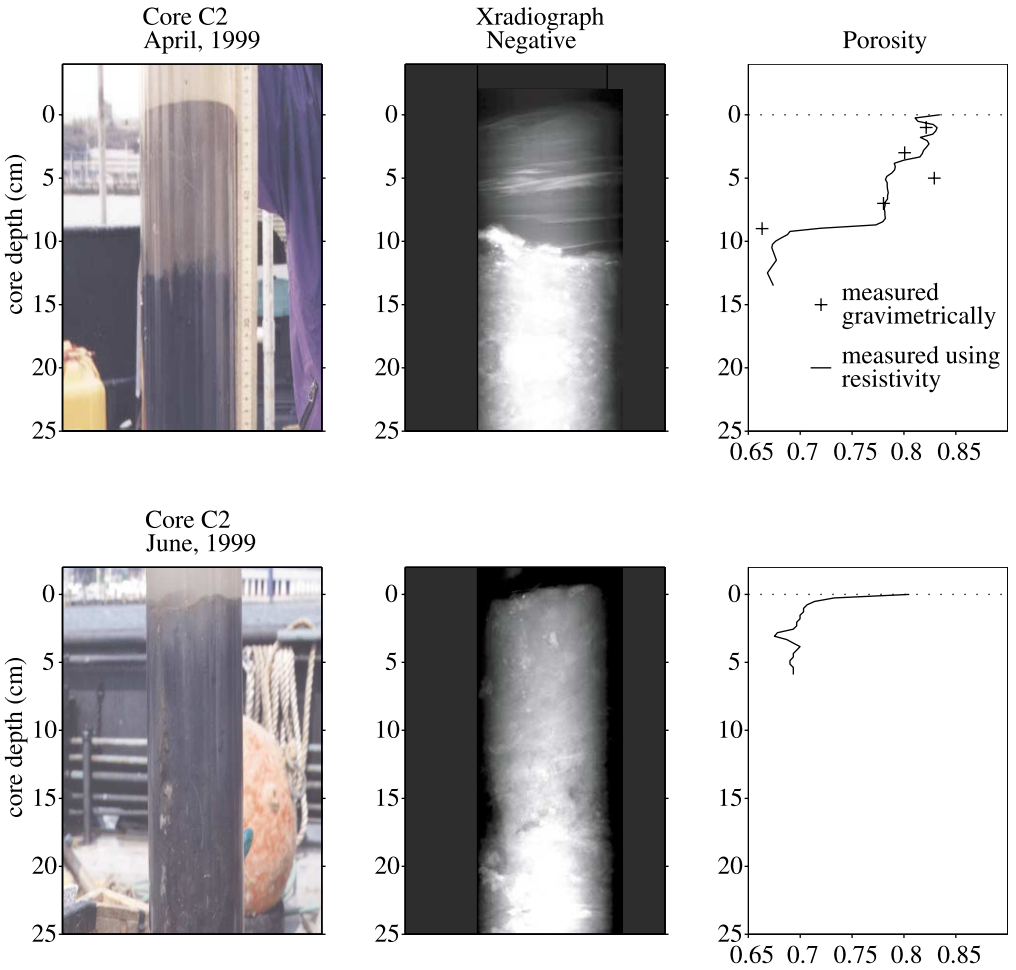

Fig. 5. Photographs, X-radiograph negatives and porosities obtained for core C-2 (located south of the ETM at 6 km) during April and June 1999. Gravimetric porosities were not measured for the June 1999 sample.

4.3. Be-7 activity profiles

Be-7 activities were measured for selected cores to obtain an approximate timescale within which the observed high porosity, olive-brown mud had been deposited. The specific activity of Be-7 in the upper 1–2 cm of bottom deposits in June of 1998, and April and June, 1999, ranged from 0.4 to 6.8 dpm/g, with an overall mean of 3.15 ± 2.0 dpm/g (Fig. 6). These surficial sediment activities are within the range previously reported for this region of the Hudson by Olsen et al. (1986) and Feng et al. (1999). Along-estuary trends in Be-7 activities were not apparent, as the upriver and seaward most sites had comparable surficial activities of 3.8 ± 0.8 dpm/g (C-4 at 34.0 km, April 1999) and 4.7 ± 0.5 dpm/g (C-1 at 1.7 km, April 1999), respectively. The narrow range of activities indicates that fluvial and oceanic waters are mixed effectively in the ETM zone, obscuring estuary-wide variations in the Be-7 inventories associated with these end-member sources (e.g. Feng et al., 1999). This observation suggests that the specific Be-7 activity of sediment arriving at the estuarine floor (i.e. initial activity) is determined largely by sedimentary processes, rather than by local variations in the water-column inventory of Be-7. For example,

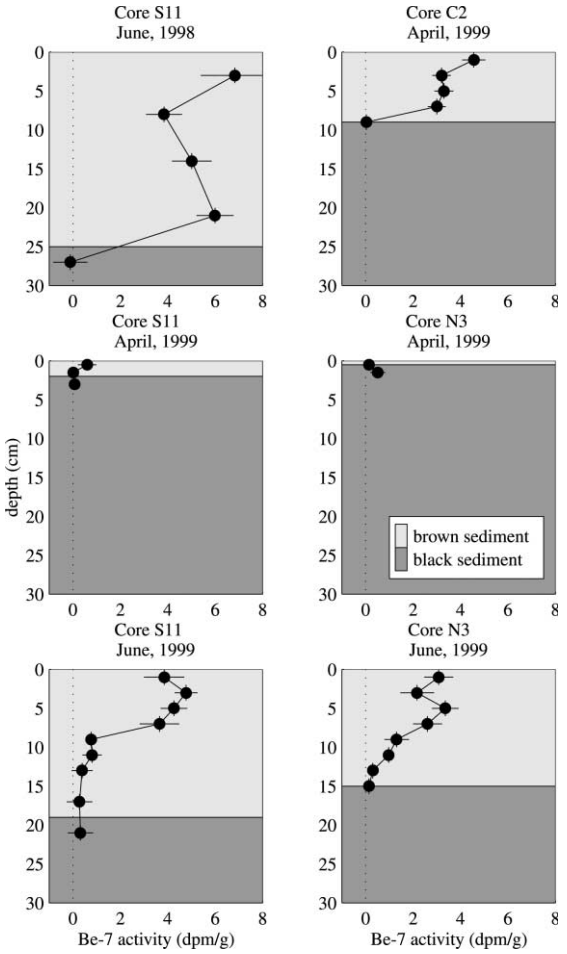

Fig. 6. Depth profiles of detectable Be-7 activity along with the thickness of olive-brown sediment.

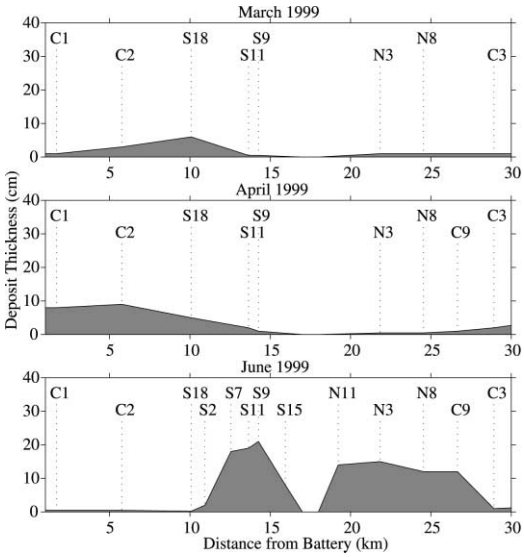

Fig. 7. Distribution of olive-brown sediment along west side of channel during the three sampling periods in 1999. Labels identify coring locations.

re-suspension scavenging–deposition cycle in shallow-marine systems have a well documented focusing effect on particle reactive radionuclides, tending to yield higher specific activities with increasing particle residence time in the water column (Baskaran et al., 1997).

In conjunction with the observed relationship between sediment color and internal sedimentary structure, the Be-7 data support a conclusion that the olive-brown, high porosity deposits are a result of very recent deposition. At core sites S-11 in June, 1998 and C-2 in April, 1999, Be-7 activity extended to the base of the olive-brown mud layer, indicating that this sediment had been in contact with the water column within about five months of sampling (based on a steady-state initial activity of 3–4 dpm/g and a 53 day half-life for Be-7). Conversely, in cores with little to no olive-brown sediment (e.g. S-11 and N-3 during April, 1999), Be-7 activities within the upper 2 cm of bottom deposits fell below minimum detection limits (<0.5 dpm/g).

Cores collected at sites S-11 and N-3 in June, 1999, contained a 19 and 15 cm thick layer of olive-brown mud, respectively (Fig. 6). Although high Be-7 activities where detected through most of these two deposits, activities did not penetrate the entire extent of the new olive-brown layers. However, since little to no olive-brown mud was observed at these two sites during the preceding sampling period in April, it can be concluded that the thick olive-brown layers observed in June were the result of recent deposition. Considering the lapse of time between the April and June cruises, the structure of the Be-7 profile may be explained by variations in initial activity during accretion, not radioactive decay. Specifically, the low Be-7 activities at the base of these recently deposited layers likely arose through the erosion of Be-7 depauperated sediment, insignificant Be-7 scavenging from the water column, and immediate deposition. Regardless of the actual sequestration process, the Be-7 data, in conjunction with the observed relationship between

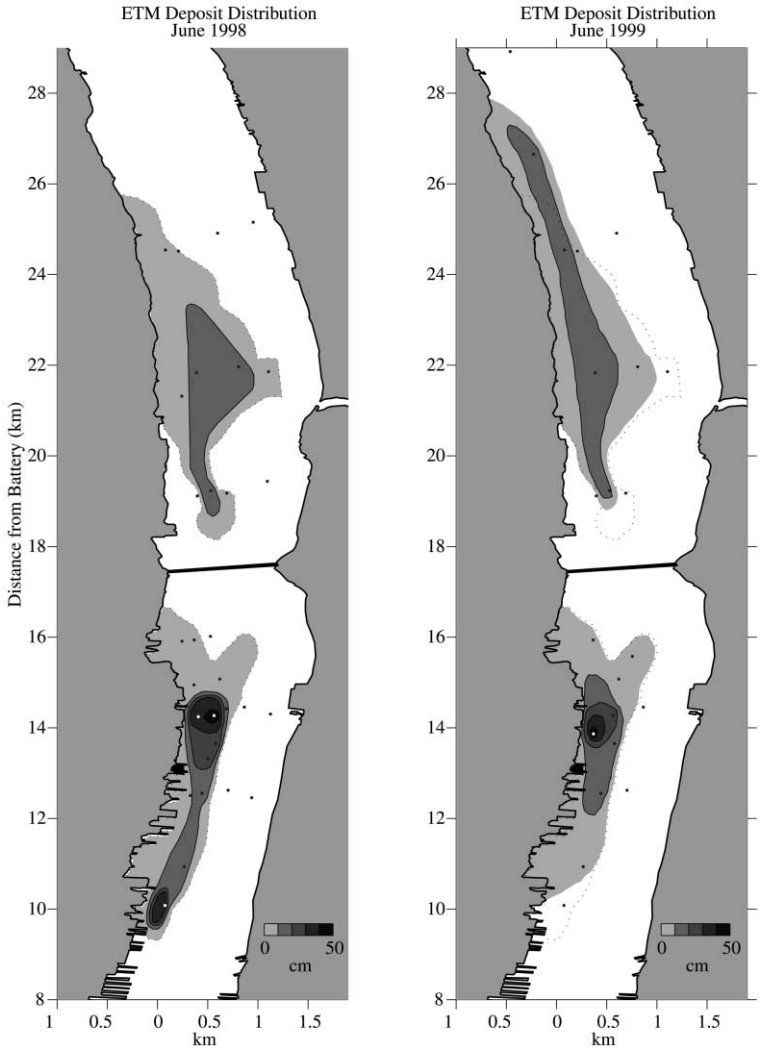

Fig. 8. Contoured depth of the 1998 and 1999 June deposits, as determined by depth of olive-brown sediment. The spatial extent of the two fine-grained deposits identified by the 1998 side-scan sonar survey are shown as a black dotted line in the figure. Black and white circles represent core locations.

sediment color, internal sedimentary structure and porosity, confirm that the observed olive-brown mud layers are the result of very recent deposition, most likely within a few months of sampling.

4.4. Seasonal sedimentation patterns and inventory

A distinct progression of deposition and sediment redistribution was observed in the Lower Hudson River estuary during this study (Fig. 7). In the seaward part of the estuary between 0 and 12 km, olive-brown mud was observed during the March and April sampling periods. This olive-brown layer increased at these seaward sites between March and April 1999, but was completely absent during the June sampling period. Between April and June, when these seaward deposits were eroded, significant sediment accumulation occurred within the two ETM deposits, between 10 and 30 km. The timing of the change in deposition pattern corresponds to the

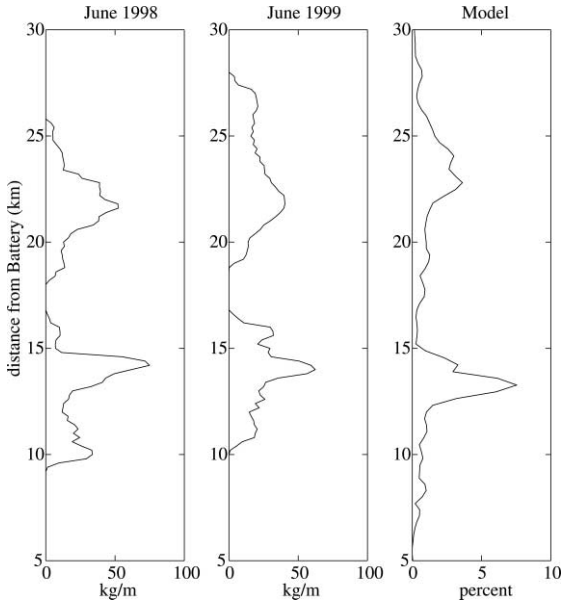

Fig. 9. Along estuary sediment distribution within the two ETM deposits. The first two panels show the distribution estimated for June of 1998 and 1999. The far right panel displays the model predictions by Geyer et al. (1998) for the distribution of sediment along the west side of the estuary, and expressed as percent of total sediment load within the model domain.

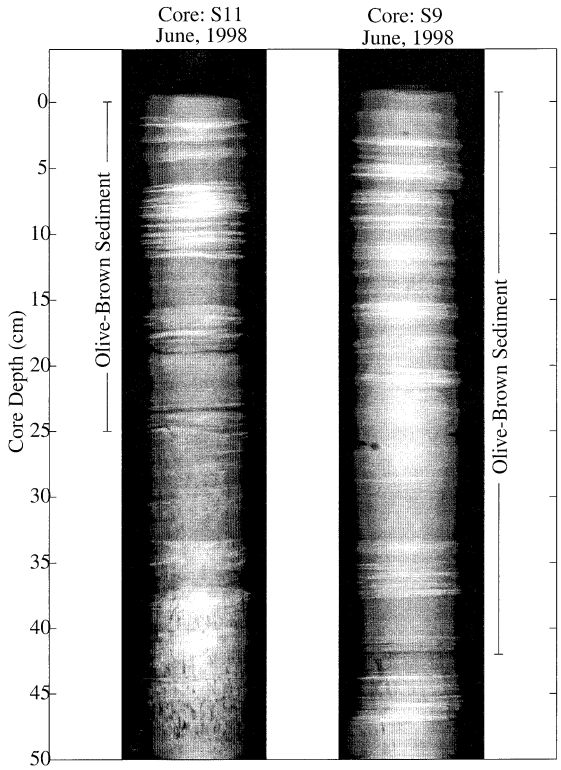

Fig. 10. X-radiograph negatives of cores collected from sites S11 and S9 during June 1998. The two cores were both located within the depocenter of the southern deposit, approximately 600 m apart from one another. The figure shows the large number of sandy silt laminae found within olive-brown sediment at these locations.

transition from high discharge to low discharge conditions. These observations are suggestive of a change in sediment trapping conditions resulting from the decrease in run-off, which allowed for a landward shift of the salinity intrusion.

The thickness of the olive-brown layer, along with the previously described transitions in internal sediment structure, porosity, and Be-7 activity were used in combination to estimate the thickness of recently deposited sediment at each of the core sites within the ETM. The spatial distribution of these deposits was estimated with guidance from the side-scan sonar record, which clearly distinguished depositional and erosional zones. Fig. 8 displays the thickness of the deposit in the ETM zone observed in June of 1998 and June of 1999. Based on a typical near-surface dry bulk density of 550 kg/m^3 and the spatial distributions of deposition displayed in Fig. 8, the estimated mass of the total ETM deposit was approximately 300 000 metric tons for both 1998 and 1999, with a comparable mass of sediment in the southern and northern depositional zones.

5. Discussion

5.1. Sediment trapping in the ETM

There is a striking similarity between the observed distribution of sediment along the west side of the estuary and the model simulations of deposition by Geyer et al. (1998), (Fig. 9). This consistency between predictions and observations of depositional patterns suggests that the model may be reproducing some of the mechanisms responsible for the observed sediment trapping. The model indicated that trapping in the southern deposit occurred as a result of frontal convergence during the ebb tide. The observed sediment depocenter at 14 km is consistent with this frontal convergence process. Water-column observations by Geyer (1995) indicate frontal formation

at this location during the ebb, consistent with the model predictions.

The numerical model indicated that trapping in the northern deposit was associated with cross-estuary, secondary circulation during the flood tide, which pushed sediment onto the shoal on the west side. The broad zone of sediment deposition between 19 and 28 km observed in June (1999) is consistent with the model prediction of the lateral convergence forming the northern deposit. Some of the details of the observed sediment distribution differ from the model, for example the broad zone of deposition around 22 km (Fig. 8). This feature may be associated either with the confluence of the Harlem River (a tidal strait) or the irregular topography in this part of the estuary. It is also noteworthy that this depositional zone is approximately one tidal excursion north of the southern deposit (based on near-bottom currents of 50–60 cm/s). A possible explanation for the enhanced deposition centered around 22 km could be the re-suspension, flood-tide transport, and deposition of sediment originally deposited at the southern ETM deposit.

Neither the observations nor the model indicate any significant sediment deposition in the vicinity of the George Washington Bridge, which falls between the northern and southern depocenters. The estuary constricts to its minimum cross-sectional area at this point, resulting in increased mixing and higher tidal velocities (Panuzio, 1965). Large bottom shear stresses associated with these high flows may prevent sediment deposition and explain the marked coarsening of bottom sediment observed in the vicinity of the bridge.

The fine-scale stratigraphy observed in the depositional zones reveals the importance of tidal processes in the sediment trapping process. Between 50 and 80 sandy-silt beds, 1–3 mm thick, were observed in the 1998, southern seasonal mud deposit within the ETM region (Fig. 10). The large number of laminae found in this olive-brown sediment and the relative dominance of tidal currents in the Lower Hudson River estuary suggest that the observed fine laminae are deposited at the tidal frequency. These layers resemble the tidal rythmites observed in other estuarine settings of similar tidal energy (Huang and Wang, 1987; Nio and Yang, 1991; Jaeger and Nittrouer, 1995). The interbedded sands and muds may reflect differences between ebb and flood deposition. Larger-scale variations in deposition would also occur as a result of spring-neap variations as well as changes in river flow, both of which alter the trapping characteristics of the estuary.

Thick (1–4 cm), homogeneous mud beds observed in cores collected from the southern depocenter appear to be associated with individual episodes of settling, based on their uniform sediment texture. These uniform muds are often spatially localized, with very little spatial coherence even at horizontal scales of several hundred meters. The spatial heterogeneity of these deposits suggest that they are not related to periods of extreme sediment loading throughout the estuary, but rather by intense, localized trapping of the horizontal sediment flux. Observations of suspended sediment in the ETM indicate that near-bottom concentrations can reach greater than 2000 mg/l during spring tides (Geyer et al., 2001). Direct, vertical deposition of the highest observed concentrations would produce roughly a 1-cm thick deposit (based on a sediment bulk density of 0.55 g/cm^3). However, if the sediment were focused in a 300-m wide frontal zone for approximately one hour, a six-fold increase in local deposition would occur (assuming complete trapping in the frontal zone with a 50 cm/s near-bottom velocity). Thus these uniform mud layers are consistent with the observed water column conditions, and may be a sedimentary record of frontal processes in the estuary assuming that sediment focusing occurs at fronts.

5.2. Fluvial influences on ETM

The seasonal progression of sedimentation in the Lower Hudson River estuary is similar to that observed for the Gironde estuary by Migniot (1971) and Allen et al. (1980), who found that the longitudinal position of sediment deposition varied as a function of freshwater flow. Migniot remarked that although the fluvial contribution to velocity was slight compared to tidal currents, its influence on the trapping conditions of the estuary was large enough to alter the location of sediment trapping by 70 km between high and low flows. The observed seasonal variations of deposition in the Hudson follow a similar pattern to the Gironde. During high discharge, the estuary is pushed toward the mouth, and sediment

trapping is favored in the lower reaches of the estuary. After river discharges have relaxed to normal levels, sediment initially deposited downstream is resuspended and transported back upstream by flood-dominated bottom currents (Geyer et al., 2001) to the ETM depositional zones. This northward transport of sediment into the ETM following the freshet is consistent with observations by Feng et al. (1999), who provided geochemical evidence that the sediment in the ETM originates from regions of higher salinity.

The estimated annual load to the estuary from the Mohawk and Upper Hudson rivers during 1998 was 560 000 metric tons, almost six times greater than the 120 000 metric tons estimated for 1999. Despite differences in annual load to the estuary, the inventory of newly deposited sediment within the ETM during June of 1998 and 1999 were found to be roughly the same, approximately 340 000 metric tons. The lack of a correlation between the seasonal sediment load and inventory indicates that there are other trapping zones within the river-estuarine system which may act as sinks for sediment during high flow years and sources to the ETM during low-flow years. Estimates of sediment flux in the Hudson in 1999 (Geyer et al., 2001) indicate that most of the sediment input was actually from the seaward direction rather than the watershed. Therefore, the excess accumulation observed within the ETM during 1999 may have originated from New York Harbor, a plausible trapping zone with its large areas of shallow, subtidal mud deposits (Coch, 1986). One possible scenario is that high flow conditions in January 1998 exported a significant fraction of the riverine load to the Harbor, which in-turn served as a source of sediment to the ETM during 1999. Meade (1972) notes that only during extreme events can sediment be exported from most U.S. East-coast estuaries, due to the effectiveness of estuarine trapping processes. The discharge event in January 1998 had a 10-year recurrence interval (based on 50 years of discharge data); events of this magnitude may be sufficient enough to provide significant sediment export past the Battery.

5.3. Long-term sediment accumulation

Olsen et al. (1978) found localized regions within the ETM of the Hudson with sediment accumulation rates as high as 30 cm/yr, based on Cs-137 dating. This high rate is consistent with the location and thickness of deposition observed within the ETM during this study. However, accumulation rates on the order of tens of cm/yr cannot be sustained for more than several decades; indeed, several years of accumulation at such rates would significantly influence the bathymetry and hydrodynamics of the estuary. An inspection of historical bathymetric data (1865, 1930, and 1998; Geyer et al., 2001) for the ETM region indicates no significant sediment accumulation, with the exception of localized effects caused by channel dredging. Therefore, natural sediment deposition and erosion processes appear to maintain an equilibrium condition in the ETM region, at least on centennial timescales. This evidence suggests that large depositional events on the order of 1998 and 1999 are likely balanced in the long-term by comparable erosion events.

As noted above, it is likely that significant sediment export from the estuary only occurs during high discharge events. The extreme discharge event in January 1998 (10 year reoccurrence interval) may have caused intense erosion within the ETM region. The duration of the 1998 flood event was approximately 5 days; in order for the erosion to be significant in the annual sediment budget, roughly 1–3 cm would have to be eroded each tidal cycle for the duration of this event. If this erosional event were only to occur every 10 years, the erosion rate would have to be 10–30 cm per tidal cycle. These latter erosion rates are an order of magnitude higher than have been observed in the Hudson (Geyer, 1995), but perhaps the extreme conditions associated with floods could profoundly influence the erosion rate. This study does not lend support to this interpretation of the role of extreme events, because it provides no direct observations of sediment erosion. Whether these erosion and export events occur annually or much less frequently is a topic for further research.

6. Summary

1. Two distinct zones of rapid sediment deposition in the Hudson ETM region were revealed through sediment coring and side-scan sonar surveys. The observations indicate a seasonal progression in the

spatial distribution of sedimentation: sediment accumulates near the mouth during the spring freshet period, and as the freshet abates, this new sediment is eroded and re-deposited further landward, in the ETM zone of the estuary. This landward shift in deposition is consistent with the landward shift in the salinity intrusion and the associated sediment trapping processes.

2. The sediment input from the watershed was estimated to be more than five times greater in 1998 than in 1999, yet the observed sediment accumulation in the ETM region was similar in both years. This discrepancy indicates that there are other zones of sediment trapping that acted as a sink for sediment in 1998 and as a source in 1999. Observations of sediment flux (Geyer et al., 2001) suggest that this sediment reservoir is to the south of the Hudson in New York Harbor. A plausible scenario that explains the observed sediment distributions is that the large flood during January 1998 caused significant erosion within the ETM and export of sediment to the harbor. Following the April 1998 freshet, an estimated 300 000 metric tons of sediment was transported to the ETM, but there still remained a pool of erodible sediment in the harbor. Following the 1999 freshet, again there was a landward transport of approximately 300 000 tons of sediment, much of which may have been derived from the large sediment transport event of January 1998.
3. The along-estuary distribution of the ETM deposits is consistent with numerical model predictions of Geyer et al. (1998). The model indicates that the sediment deposition in the southern part of the ETM results from trapping in an ebb-tide frontal zone, consistent with the observed high rates of sedimentation in this part of the estuary. The model indicates a more elongated trapping zone along the west side of the estuary in the northern portion of the ETM, caused by transverse near-bottom currents during the flood tide. The sediment deposition pattern during the 1998 and 1999 observations are consistent with those model results. However, the spatial structure of the northern deposit is more complex than predicted by the model, perhaps because of the confluence of the Harlem River or local complexities in channel morphology.
4. This study did not address the issue of erosion, although the long-term sediment budget of the estuary requires that erosion from the ETM occur either annually or during less frequent, extreme events, to maintain the equilibrium channel morphology. Historical records of channel morphology indicate that the ETM-region of the estuary is in approximate equilibrium on a 100-year timescale, notwithstanding recent dredging activity. If erosion events occurred mainly in association with 10-year discharge events, they would require erosion rates an order-of-magnitude larger than have been observed in the estuary. The question of how the sediment balance is maintained on interannual to centennial timescales is the subject of ongoing research.

Acknowledgements

The authors thank Mike Bothner, Marilyn ten Brink, and Larry Poppe from the USGS Woods Hole Field Center for the use of their equipment and facilities in the collection and processing of sediment samples. The acquisition of side-scan data benefited from the help of Michael Bruno, Terry Donoghue and Wayne Spencer. This work was supported by the Hudson River Foundation Grant 004-98A, the Office of Naval Research Processes Program Grant N00014-99-1-0039, and WHOI contribution 10471.

References

Abood, K.A., 1974. Circulation in the Hudson Estuary. Ann. NY Acad. Sci. 250, 39–111.

Allen, G.P., Salmon, J.C., Bassoullet, P., Du Penhoat, Y., De Grandpre, C., 1980. Effects of tides on mixing and suspended sediment transport in macrotidal estuaries. Sedim. Geol. 26, 69–90.

Baskaran, M.M., Ravichandran, M., Bianchi, T.S., 1997. Cycling of Be-7 and Pb-210 in a high DOC, shallow, turbid estuary of south-east Texas. Estuarine, Coast. Shelf Sci. 45, 165–176.

Berner, R.A., 1980. Early Diagenesis: A Theoretical Approach. Princeton University Press, Princeton, NJ pp. 15–55.

Bothner, M., Gill, P., Boothman, W., Taylor, B., Karl, H., 1997. Chemical and textural characteristics of sediments at an EPA reference site for dredged material on the continental slope SW of the Farallon Islands. Open-File Report 97-87, US Geological Survey, Woods Hole Field Center.

Coch, N.K., 1986. Sediment characteristics and facies distributions in the Hudson system. Northeastern Geol. 8, 109–129.

Danforth, W., 1997. Xsonar/Showimage: a complete system for rapid sidescan sonar processing and display. Open-File Report 97-686, US Geological Survey, Woods Hole Field Center, Quissett Campus, Woods Hole, MA, 02543.

Dowling, J.J., 1990. Estimating porosity of partially saturated sediments. Engng Geol. 29, 139–147.

Feng, H., Cochran, J.K., Hirschberg, D.J., Wilson, R.E., 1998. Small-scale spatial variations on natural radionuclide and trace metal distributions in the sediment from the Hudson River estuary. Estuaries 21, 263–280.

Feng, H., Cochran, J.K., Hirschberg, D.J., 1999. Th-234 and Be-7 as tracers for the sources of particles to the turbidity maximum of the Hudson River estuary. Estuarine, Coast. Shelf Sci. 49, 629–645.

Flood, R.D., Bokuniewicz, H.J., 1986. Bottom morphology in the Hudson River estuary and New York Harbor. Northeastern Geol. 8, 130–140.

Folk, R.L., 1980. Petrology of Sedimentary Rocks. Hemphill Publishing Company, Austin, TX, pp. 15–37.

Geyer, W.R., 1993. The importance of suppression of turbulence by stratification on the estuarine turbidity maximum. Estuaries 16, 113–125.

Geyer, W.R., 1995. Final report: Particle trapping in the Lower Hudson Estuary. Submitted to Hudson River Foundation (April 1995).

Geyer, W.R., Woodruff, J.D., Traykovski, 2001. Sediment trapping and transport in the Hudson River Estuaries, in press.

Geyer, W.R., Signell, R.P., Kineke, G.C., 1998. Lateral trapping of sediment in a partially mixed estuary. Proceedings of the 8th International Biennial Conference on Physics of Estuaries and Coastal Seas, pp. 115–124.

Geyer, W.R., Trowbridge, J., Bowen, M., 2000. The dynamics of a partially mixtured estuary. J. Phys. Oceanogr. 30, 2035–2048.

Gibbs, R.J., Tshudy, D.M., Konwar, L., Martin, J.M., 1989. Coagulation and transport of sediment in the Gironde Estuary. Sedimentology 36, 987–999.

Glangeaud, L., 1938. Transport et sedimentation dans l'estuaire de la Gironde (caracteres petrographiques des formations fluviatiles, suamatres, littorales et neritiques). Bull. Geol. Soc. Fr. 8, 599–630.

Grabemann, I., Uncles, R.J., Krause, G., Stephens, J.A., 1997. Behavior of turbidity maxima in the Tamar (UK) and Weser (F.R.G.) Estuaries. Estuarine, Coast. Shelf Sci. 45, 235–246.

Hirschberg, D.J., Bokuniewicz, H.J., 1991. Measurements of water, temperature, salinity and suspended sediment concentrations along the axis of the Hudson River estuary 1980–1981. Special Data Report: Marine Sciences Research Center, State University of New York, Report 11, Reference 91-14.

Hirschberg, D.J., Chin, P., Feng, H., Cochran, J.K., 1996. Dynamics of sediment and contaminant transport in the Hudson River Estuary: evidence from sediment distributions of naturally occurring radionuclides. Estuaries 19, 931–949.

Huan-ting, S., Hui-fang, Z., Zhi-chang, M., 1982. Circulation of the Chang Jiang Estuary and its effect on the transport of sediment. In: Kennedy, V. (Ed.), Estuarine Comparisons. Academic Press, New York, pp. 676–677.

Huang, N., Wang, G., 1987. The new criteria of ancient tidal sediments–tidal cycle sequence. Acta Sedimentol. Sinica 5, 39–44.

Jaeger, J.M., Nittrouer, C.A., 1995. Tidal controls on the formation of fine-scale sedimentary strata near the Amazon River mouth. Mar. Geol. 125, 259–281.

Larsen, I.L., Cutshall, N.H., 1981. Direct determination of Be-7 in sediments. Earth Planet. Sci. Lett. 54, 379–384.

Lick, W., Huang, H., 1993. Flocculation and the physical properties of flocs. In: Mehta, A.J. (Ed.), Nearshore and Estuarine Cohesive Sediment Transport. American Geophysical Union, Washington, DC, pp. 21–39.

Meade, R.H., 1969. Landward transport of bottom sediments in estuaries of the Atlantic Coastal Plain. J. Sedim. Petrol. 39, 222–234.

Meade, R.H., 1972. Transport and deposition of sediments in estuaries. Geol. Soc. Am. Mem. 133, 91–120.

Migniot, C., 1971. L'evolution de la Gironde au cours des temps. Inst. Geol. Bassin d'Aquitaine Bull. 11, 221–281.

Nichols, M.M., 1977. Response and recovery of an estuary following a river flood. J. Sedim. Petrol. 47, 1171–1186.

Nichols, M.M., Johnson, G.H., Peebles, P.C., 1991. Modern sediments and facies model for a microtidal coastal plain estuary, the James Estuary, Virginia. J. Sedim. Petrol. 61, 883–899.

Nio, S.D., Yang, C., 1991. Diagnostic attributes of clastic tidal deposits; a review. In: Smith, R. (Ed.), Clastic Tidal Sedimentology. Canadian Society of Petroleum Geologists Memoir 16, pp. 3–27.

Olsen, C.B., 1979. Radionuclides, sedimentation and the accumulation of pollutants in the Hudson Estuary. PhD Thesis, Columbia University.

Olsen, C.B., Simpson, H.J., Bopp, R.F., Williams, S.C., Peng, T.H., Deck, B.L., 1978. A geochemical analysis of the sediments and sedimentation in the Hudson Estuary. J. Sedim. Petrol. 48, 401–418.

Olsen, C.B., Simpson, H.J., Peng, T.H., Bopp, R.F., Trier, R.M., 1981. Sediment mixing and accumulation rate effects on radionuclide depth profiles in the Hudson Estuary sediments. J. Geophys. Res. 86, 11020–11028.

Olsen, C.B., Larsen, I.L., Lowry, P.D., Cutshall, N.H., Nichols, M.M., 1986. Geochemistry and deposition of Be-7 in river-estuarine and coastal waters. J. Geophys. Res. 91, 896–908.

Panuzio, F.L., 1965. Lower Hudson River siltation. Proceedings of the Ferral InterAgency Sedimentation Conference. Agriculture Research Service, pp. 512–550, Misc. Publ. 970.

Postma, H., 1967. Sediment transport and sedimentation in the estuarine environment. In: Lauff, G.H. (Ed.), Estuaries. American Association for the Advancement of Science, Washington, DC, pp. 158–179.

Woodruff, J.D., 1999. Sediment deposition in the Lower Hudson River estuary. Masters Thesis, Massachusetts Institute of Technology/Woods Hole Oceanographic Institution.